Scripta Materialia 110 (2016) 33–36

Contents lists available at ScienceDirect

Scripta Materialia

journal homepage: www.elsevier.com/locate/scriptamat

Substrate topography guides pore morphology evolution in nanoporous gold thin films

Christopher A.R. Chapman [a], Pallavi Daggumati [b], Shannon C. Gott [c], Masaru P. Rao [c,d,e], Erkin Seker [b,*]

[a] Department of Biomedical Engineering, University of California – Davis, Davis, CA 95616, USA
[b] Electrical & Computer Engineering, University of California – Davis, Davis, CA 95616, USA
[c] Department of Mechanical Engineering, University of California – Riverside, Riverside, CA 92521, USA
[d] Department of Bioengineering, University of California – Riverside, Riverside, CA 92521, USA
[e] Materials Science and Engineering Program, University of California – Riverside, Riverside, CA 92521, USA

ARTICLE INFO

Article history:
Received 19 June 2015
Revised 22 July 2015
Accepted 28 July 2015
Available online 3 August 2015

Keywords:
Nanoporous material
Annealing
Dealloying
Fracture
Microfabrication

ABSTRACT

This paper illustrates the effect of substrate topography on morphology evolution in nanoporous gold (np-Au) thin films. One micron-high silicon ridges with widths varying between 150 nm and 50 μm were fabricated and coated with 500 nm-thick np-Au films obtained by dealloying sputtered gold–silver alloy films. Analysis of scanning electron micrographs of the np-Au films following dealloying and thermal annealing revealed two distinct regimes where the ratio of film thickness to ridge width determines the morphological evolution of np-Au films.

Nanoporous gold (np-Au), produced by selective dissolution of silver from a gold–silver alloy (known as *dealloying*) [1], is an emerging material that exhibits many desirable properties, including high electrical conductivity [2,3], catalytic activity [4,5], tunable pore morphology [3,6–8], and compatibility with conventional micropatterning techniques [2,3,9,10]. These properties translate into various applications, including multifunctional biomedical device coatings [2,11,12], bioanalytical sensors [13–15], catalytic applications [4,5], as well as fundamental studies of structure–property relationships [10,16–20]. As precise control of material morphology (e.g., pore size) is essential for these applications, it is necessary to have an understanding of parameters that influence morphology evolution. To that end, previous studies have explored the effect of alloy composition [17], dealloying method [21,22], and post-processing techniques [6] on pore morphology. However, the effect of substrate topography on morphology evolution still remains largely unknown. As np-Au thin films supported on substrates benefit from the versatility of micropatterning (e.g., photolithography) and deposition techniques (e.g., physical vapor deposition, electroplating) for integration with devices, the role of substrate topography becomes increasingly important. The objective of this paper is therefore to address this knowledge gap by systematically investigating the role of surface topography in morphology evolution. Specifically, we employed microridge arrays (MRAs) of textured silicon substrates coated with sub-micron-thick np-Au films for studying morphological evolution of np-Au films on multiple ridge widths and a smooth (non-textured) surface on a single chip (Fig. 1).

Silicon MRAs were fabricated by photolithographic patterning with a deep ultraviolet (DUV) stepper (PAS 5500/300, ASML), followed by pattern transfer to the underlying silicon substrate with fluorine-based dry etching (SLR 770 ICP, Unaxis), and finally photoresist (PR) removal by oxygen plasma (PE-IIA, Technics). A portion of the chip was not patterned to serve as a smooth control surface, labeled as *blank* (Fig. 1). Ridge profile and groove depth were characterized by cross-sectional images of test MRAs obtained by sectioning the chips with a focused ion beam system (CrossBeam XB1540, Carl Zeiss) and imaging them with a scanning electron microscope (SEM) (SUPRA 55, Carl Zeiss), as previously described [23]. The MRA fabrication process yields excellent agreement between the dimensions of expected and fabricated ridges [23]. Np-Au films were prepared as described previously [9]. Briefly, the silicon MRAs were cleaned by 10 min-long immersion in a freshly prepared Piranha solution, composed of 1:4 volumetric ratio of hydrogen peroxide (30%) to sulfuric acid (96%). The array chips were subsequently rinsed in deionized (DI) water and dried under nitrogen flow prior to metal deposition with a

* Corresponding author.
E-mail address: eseker@ucdavis.edu (E. Seker).

http://dx.doi.org/10.1016/j.scriptamat.2015.07.039
1359-6462/

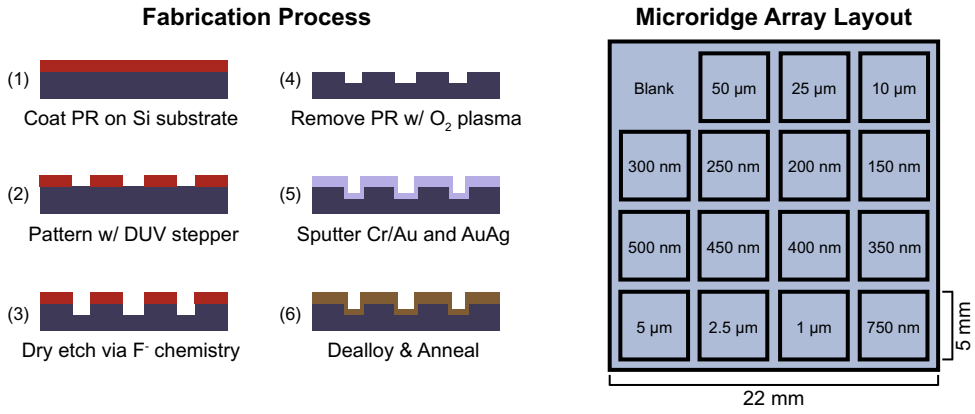

Fig. 1. Summary of microfabrication steps for producing the silicon MRAs used as a substrate for np-Au thin film deposition. Each square region is covered by parallel ridges of equal width and spacing with the superimposed dimension.

magneto-sputtering system (Kurt J. Lesker). First, a 160 nm-thick chrome layer was sputtered to promote adhesion between the silicon substrate and the subsequent metallic layers. Next, 80 nm-thick seed layer of gold was sputtered and finally silver and gold were co-sputtered from different targets to obtain a 600 nm-thick alloy layer. All depositions were performed successively (without breaking the vacuum) in argon at a pressure of 10 mTorr. The composition of the alloy was 64% Ag and 36% Au (at.%) as determined by X-ray energy dispersive spectroscopy (Oxford Instruments). The samples were dealloyed in 70% nitric acid at 55 °C for 3 min and additional 12 min (total dealloying time of 15 min) to produce the np-Au films. In order to assess the effect of annealing on the pore area evolution, dealloyed chips were thermally treated for 3 min at 325 °C in a rapid thermal annealer (Accu Thermo 610).

The np-Au film morphology on the ridges was acquired with a SEM (Nova NanoSEM430, FEI) following three steps during np-Au processing: three minutes of dealloying, additional 12 min of dealloying, and three minutes of annealing at 325 °C. The SEM images (image field of 2.5 μm by 3 μm) were analyzed with custom ImageJ (National Institutes of Health shareware) scripts to obtain the areas of each void (i.e., pores and cracks). Briefly, each image was segmented to differentiate between pores/cracks (dark) and ligaments (light) in the images (Fig. 2 and Supplementary Material) [9]. The cracks were defined as the surface features in top 5% of the pore area distributions for each case (Figs. S1–S3). SEM images from three different regions on each ridge width, away from the ridge edges, were analyzed to calculate the median pore area/crack size (data point) and the corresponding standard error (error bar). The percent lateral shrinkage in the np-Au films on the ridges with respect to the initial width of the alloy were calculated from the low-magnification SEM images of the films on ridges (Fig. 2 insets). Details of the fabrication and characterization methods can be found in Supplementary Material.

The underlying mechanism that leads to the open-pore morphology of np-Au with interconnected ligaments is the interplay between two processes: (i) roughening driven by dissolution of silver from the alloy, and (ii) smoothing/coarsening driven by enhanced surface diffusion of gold atoms at the metal-electrolyte interface [1]. After the three-minute dealloying, the np-Au films displayed smaller pore areas on each ridge (Fig. 2A) in comparison to the typical dealloying time of 15 min (Fig. 2B). It is expected that the short dealloying duration is sufficient for silver dissolution and porosity formation, but not long enough to produce significant surface diffusion-driven coarsening [8]. After the 15-min dealloying, differences in pore morphologies for each ridge width became

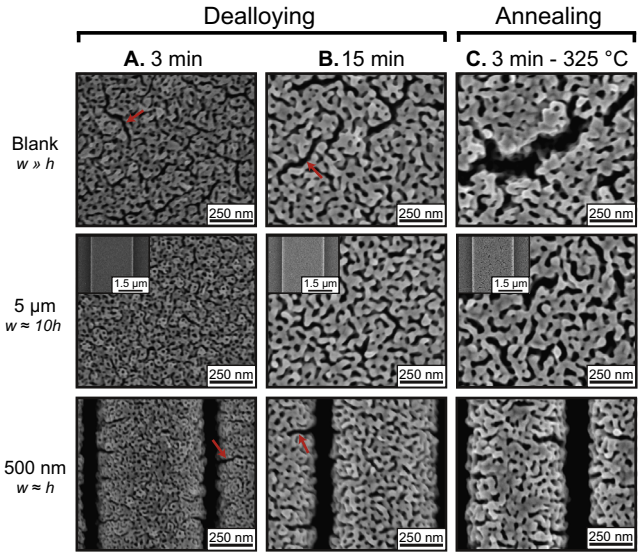

Fig. 2. SEM images illustrating morphology evolution in np-Au films on three representative surface topographies after dealloying (A and B) and annealing (C). relationship between film thickness, *h*, and the ridge width, *w*, dictates the nature of pore coarsening and crack formation. Initial crack formations during dealloying are highlighted by red arrows. The insets are low-magnification images of the films on 5 μm-wide ridges. (For interpretation of the references to colour in this figure legend, the reader is referred to the web version of this article.)

more apparent. Pore areas on both 5 μm and 10 μm ridges (also on the *blank* to a lesser extent) became significantly increased (Fig. 3A), compared to all other ridge widths. The np-Au-coated MRAs were then annealed at 325 °C for three minutes to enhance surface-diffusion of gold atoms, which is typically used for obtaining coarser morphologies [6,7]. As for the case of dealloyed samples, the pore areas on 5 μm and 10 μm ridges as well as the *blank* control surface (denoted as ∞) remained much larger ($\sim 2\times$) than the narrower ridges (Figs. 2 and 3A). Two regimes of pore morphology evolution with respect to ridge width become visible (Fig. 2A). Below a *critical width* positioned between ridge widths of 1 μm and 2.5 μm, pore evolution is hindered ($\sim 2\times$ increase from 3-min dealloying to annealing). Above this transition width, more significant pore coarsening ($\sim 4\times$ increase for 5 μm and 10 μm, $3\times$ increase for *blank*) is present. This is attributed to np-Au thin film mechanics in relation to the ratio of film thickness, *h*, to ridge width, *w*, which will be discussed later in the context of additional morphological and geometric phenomena.